physiologia

MDPI

Brief Report

The Effects of Spermidine on Functional and Transcriptomic Markers in Human Primary Keratinocytes

Derick A. Anglin, Madison L. Mattingly, Nicholas J. Kontos and Michael D. Roberts *

School of Kinesiology, Auburn University, 301 Wire Road, Auburn, AL 36849, USA; daa0017@auburn.edi (D.A.A.); mlm0139@auburn.edu (M.L.M.); njk0013@auburn.edu (N.J.K.)
* Correspondence: mdr0024@auburn.edu

Abstract

Recent enthusiasm has surrounded the homeostatic roles that polyamines have in a variety of cell types. Thus, the purpose of this exploratory in vitro study was to determine how spermidine (SPD), a polyamine commonly consumed as a nutritional supplement, affected general markers of cellular health and function in human primary epidermal keratinocytes. Commercial HEKa cells were seeded onto either six-well (transcriptomics and immunoblotting) or 96-well culture plates (viability, ATP, and JC-1 assays) and cultured to ~90+% confluency through complete growth media (CGM) changes every 48 h. Once cells reached this level of growth, treatments included either CGM + phosphate-buffered saline (PBS control, or CTL), CGM + 1 μM SPD, and CGM + 10 μM SPD for either 6 or 24 h depending upon the outcome being assessed. Cellular ATP levels were not significantly affected by 1 μM or 10 μM SPD treatments lasting 24 h. However, cell counts were 9% greater ($p = 0.007$) when comparing 24 h 10 μM versus CTL treatments indicating increased cell viability. Transcriptomic analyses indicated that 6 h treatments with 10 μM SPD significantly altered 162 transcripts versus non-treated CTL cells (65 up-regulated and 97 down-regulated, $p < 0.01$). Four pathways were predicted to be enriched based on differential gene expression including protein deubiquitination (GO:0016579), membrane lipid biosynthesis (GO:0046467), DNA metabolic process (GO:0006259), and cell cycle process (GO:0022402). Additionally, the HR gene (essential for keratinocyte hair follicle formation) was significantly up-regulated at the mRNA level with 6 h 10 μM SPD, and immunoblotting confirmed a 96% increase in protein levels with 24 h 10 μM SPD treatments, albeit this did not reach statistical significance ($p = 0.102$). Pan-keratin protein content was also 60% greater in the 1 μM and 10 μM 24 h treatments than CTL ($p \leq 0.029$). Finally, although select markers of mitochondrial content and biogenesis were not significantly altered with 6 h and 24 h treatments, mitochondrial membrane potential (an aspect of mitochondrial function) was 84% greater with 24 h 1 μM versus CTL ($p < 0.001$). In conclusion, these preliminary screening experiments in unperturbed human keratinocytes suggest that exogenous SPD positively affects various aspects of homeostasis by stimulating transcriptomic and functional alterations (e.g., increased cell viability and enhanced keratinocyte protein levels).

Keywords: keratinocytes; spermidine; keratin; transcriptomics

check for updates

Academic Editors: Ana B Rodríguez Moratinos and Stella M. Valenzuela

Received: 26 July 2025
Revised: 22 September 2025
Accepted: 29 September 2025
Published: 15 October 2025

Citation: Anglin, D.A.; Mattingly, M.L.; Kontos, N.J.; Roberts, M.D. The Effects of Spermidine on Functional and Transcriptomic Markers in Human Primary Keratinocytes. *Physiologia* **2025**, *5*, 43. https://doi.org/10.3390/physiologia5040043

Copyright: © 2025 by the authors. Licensee MDPI, Basel, Switzerland. This article is an open access article distributed under the terms and conditions of the Creative Commons Attribution (CC BY) license (https://creativecommons.org/licenses/by/4.0/).

1. Introduction

The integumentary system comprises skin, hair, and nails [1]. The epidermal skin layer is primarily composed of keratinocytes as well as melanocytes and specialized immune

(Langerhans) cells that continually renew to form a protective barrier [2]. Hair follicles are epidermal invaginations that extend into the underlying dermal layer [2]. A variety of cell types (e.g., matrix cells along with hair follicle and melanocyte stem cells) exist in a complex microenvironment that makes up the hair follicle [3], whereas other cell types (e.g., medullary, cortical, cuticular) are differentiated products of matrix cell division that form the hair shaft structure. Nail-producing cells in the nail matrix proliferate and harden into protective nail plates. Despite their structural differences, these three components share similarities in that they all produce keratin as their primary structural protein, serve protective functions for the body, and undergo continuous cycles of growth and renewal.

Polyamines are small, positively charged cellular metabolites found in micromolar concentrations and include putrescine, spermidine (SPD), and spermine [4]. These molecules are synthesized from either L-ornithine or through the decarboxylation of amino acids. Two key enzymes regulate polyamine synthesis including ornithine decarboxylase (ODC) and S-adenosylmethionine decarboxylase (SAMDC) [5]. Like other cellular metabolites (e.g., NAD^+ and creatine), polyamine concentrations (notably SPD) decrease with age [6]. Indeed, dietary sources such as cheese, shellfish, and certain plants (e.g., soybeans and grains) provide a source of polyamines [5]. However, cellular levels are maintained through exogenous intake along with intracellular biosynthesis and production from certain gut microbiota [7]. Initial research in yeast suggested that exogenous SPD administration extends lifespan through epigenetic and redox-related mechanisms [8]. Since then, several studies have supported that SPD is involved in a variety of cellular processes including the regulation of growth, proliferation, and redox balance [4,9,10]. SPD is also involved in regulating homeostatic autophagy in various cell types [10]. Additionally, SPD serves as the sole substrate for the hypusination of eukaryotic initiation factor 5A (eIF5A), a post-translational modification essential for protein synthesis, mitochondrial function, and cellular proliferation [11].

Interestingly, exogenous SPD administration has also been shown to positively impact the integumentary system. For instance, the topical administration of SPD in rodents has been reported to enhance skin wound repair [12] and reduce skin flap necrosis [13]. Hynd and Nancarrow reported that the pharmacological inhibition of ODC and SAMDC reduced wool follicle formation in vitro, and that the addition of SPD reversed these effects [14]. Ramot et al. [15] examined the effects of micromolar spermidine doses on human scalp organ cultures and hair follicle epithelial stem cells. These authors reported that in vitro SPD treatments up-regulated keratin gene expression and increased stem cell proliferation. These same researchers subsequently performed a placebo-controlled study to determine that SPD supplementation over a three-month period mechanistically combats hair loss through an anagen-prolonging effect on hair follicles [15].

Given the putative roles that SPD has in the integumentary system, the purpose of this exploratory study was to determine how SPD affected pan keratin protein expression, cell viability, global mRNA expression, and other indices of cellular health in primary human keratinocytes. Per prior literature, we hypothesized that SPD would increase pan keratin production and markers suggestive of enhanced cellular function and health in keratinocytes in vitro. We did not adopt an a priori hypothesis on how SPD would affect global gene expression or other exploratory outcomes (e.g., mitochondrial biogenesis and function markers).

2. Results

2.1. Effects of 24 h SPD Treatments on Cellular ATP and Viability

Figure 1 contains 24 H treatment data for CTL as well as lower (1 μM) and higher (10 μM) SPD doses. Although cellular ATP levels were not affected by treatments

(Figure 1a), relative cell counts were significantly greater with 10 μM treatments than the CTL condition (9%, $p = 0.007$; Figure 1b).

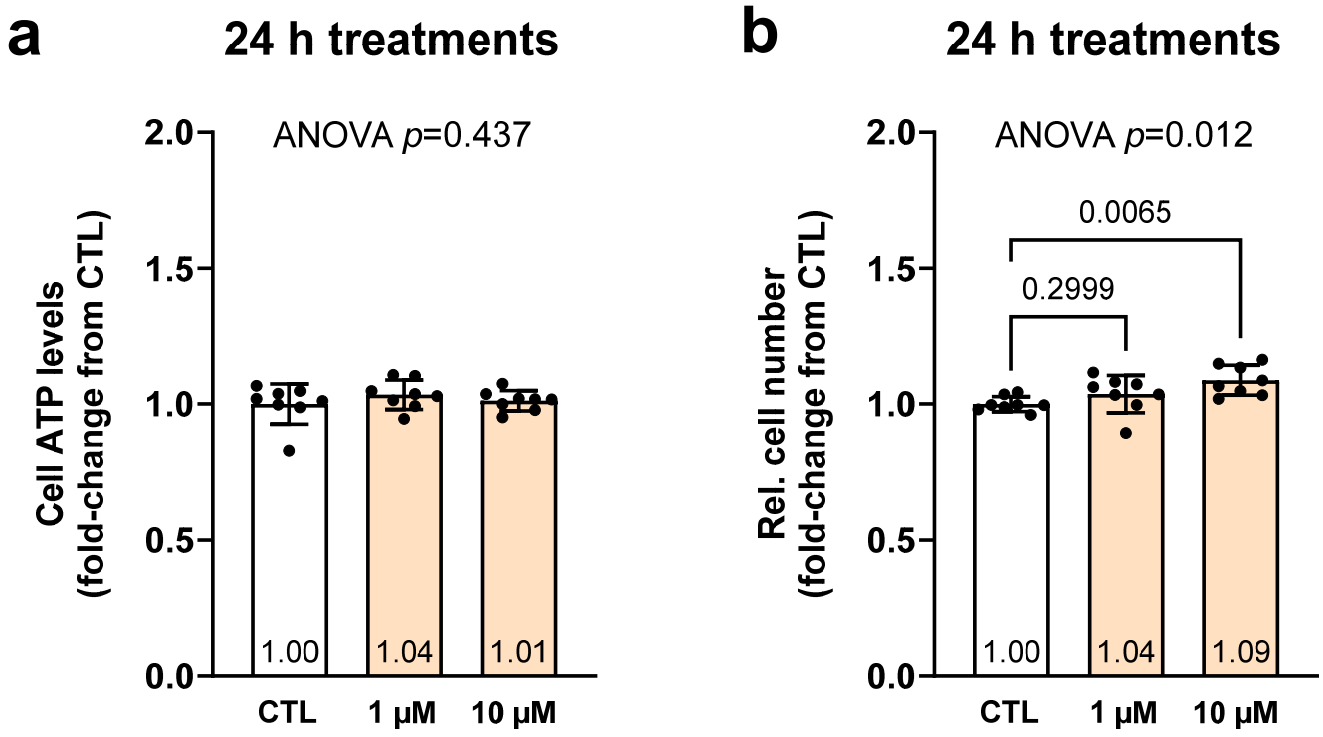


Figure 1. Effects of 24 h SPD treatments on cellular ATP and viability. Legend: These data illustrate the effects of lower (1 μM) and higher (10 μM) spermidine (SPD) treatments as well as non-treated cell (CTL) cellular ATP levels (**a**) and relative cell number (**b**). Bars are laid out as mean ± standard deviation values with individual replicate values (n = 8 per treatment) being presented as dots, and mean values are presented at the bottom of each bar. Note, white bars are CTL treatment data and orange bars are SPD treatment data.

2.2. Effects of 6 h 10 μM SPD Treatments on Transcriptomic Outcomes

We next aimed to determine how 6 h (acute) 10 μM SPD treatments affected global mRNA expression patterns in keratinocytes. Please note that Benjamini–Hochberg false discovery rate analysis indicated that no target obtained an FDR-adjusted p-value of <0.10. However, according to our $p < 0.01$ threshold, SPD significantly increased 65 mRNAs and significantly decreased 97 mRNAs; note that the top 20 respective transcripts in these classes are presented in Figure 2a,b.

When querying the 162 differentially altered transcripts with 10 μM SPD treatments, PANTHER GO-Slim Biological Processes that were predicted to be significantly enriched according to the statistical overrepresentation test are presented in Table 1. After adjusting pathway analysis for more statistical stringency ($p < 0.01$) and removing redundant parent Gene Ontology (GO) biological processes, four pathways were predicted to be enriched based on differential gene expression including protein deubiquitination (GO:0016579), membrane lipid biosynthesis (GO:0046467), DNA metabolic process (GO:0006259), and cell cycle process (GO:0022402). No down-regulated pathways were predicted to be enriched.

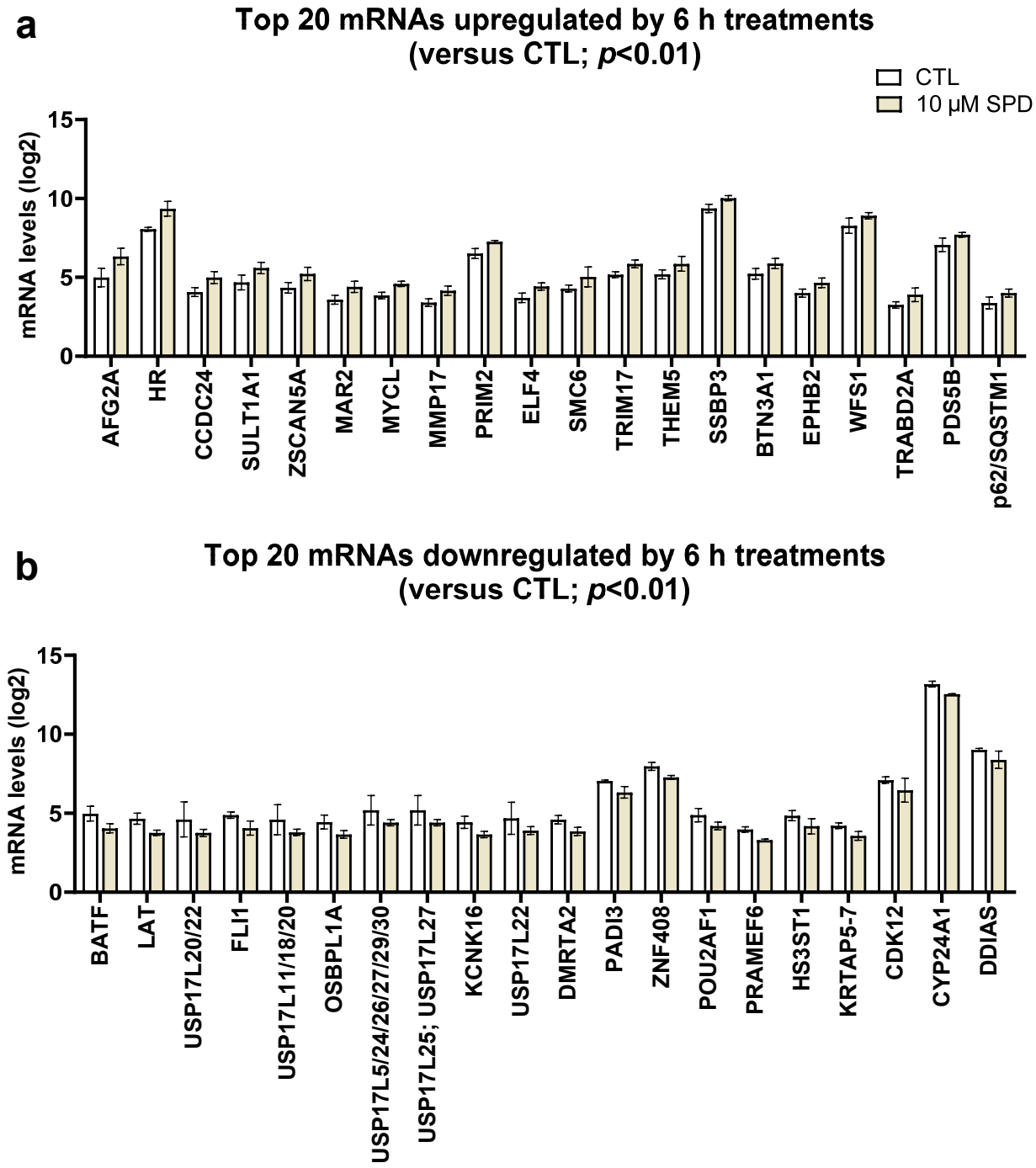


Figure 2. Effects of 6 h 10 µM SPD treatments on keratinocyte transcriptomics. Legend: These data illustrate the effects of higher (10 µM) spermidine (SPD) treatments on the top 20 up-regulated (**a**) and top 20 down-regulated (**b**) transcripts. Bars are laid out as mean ± standard deviation values (n = 6 replicates for SPD as well as CTL cells). Note, white bars are CTL treatment data and orange bars are SPD treatment data.

2.3. Effects of 6 and 24 h SPD Treatments on Cellular Protein Outcomes

Figure 3 contains 6 and/or 24 h treatment data for CTL as well as lower (1 µM) and/or higher (10 µM) SPD doses. Pan-keratin protein content was 60% greater in the 24 h 1 µM and 10 µM treatments than the CTL condition ($p \leq 0.029$; Figure 3a). The ANOVA was not statistically significant with HR protein expression ($p = 0.193$).

Table 1. Predicted pathway enrichment based on 6 h 10 μM spermidine SPD treatments.

Pathway (GO Accession), *p*-Value	Predicted Direction	Fold-Enrichment	Genes in Pathway Altered, Fold-Change (*p* = Value)
Protein deubiquitination (GO:0016579), $p < 0.001$	↑	8.0	USP24, +1.45 ($p = 0.005$) USP17L22, −1.82 ($p = 0.005$) USP17L20, −1.82 ($p = 0.005$) USP26, +1.43 ($p = 0.002$) USP17L27/30, −1.73 ($p = 0.001$)
Membrane lipid biosynthetic process (GO:0046467), $p = 0.003$	↑	6.8	PIGZ, −1.30 ($p = 0.008$) SPTLC1, −1.50 ($p = 0.004$) UGCG, −1.30 ($p = 0.009$) DPM3, −1.45 ($p = 0.007$)
DNA metabolic process (GO:0006259), $p = 0.008$	↑	3.1	TOP1MT, +1.37 ($p = 0.002$) ATRX, −1.31 ($p = 0.001$) PDS5B, +1.55 ($p = 0.001$) SMC6, +1.66 ($p = 0.007$) RAD9B, +1.27 ($p = 0.009$) DNMT3B, +1.27 ($p = 0.008$) PRIM2, +1.68 ($p = 0.003$)
Cell cycle process (GO:0022402), $p = 0.009$	↑	3.0	TOP1MT, +1.37 ($p = 0.002$) CETN1, +1.24 ($p = 0.008$) PDS5B, +1.55 ($p = 0.001$) RAD9B, +1.27 ($p = 0.009$) USP26, +1.43 ($p = 0.002$) AURKC, +1.43 ($p = 0.001$) OIP5, −1.25 ($p = 0.004$)

Legend: These biological processes were predicted to be enriched based on 6 h mRNA alterations with 10 μM spermidine treatments. Note, ↑ indicates predicted up-regulation.

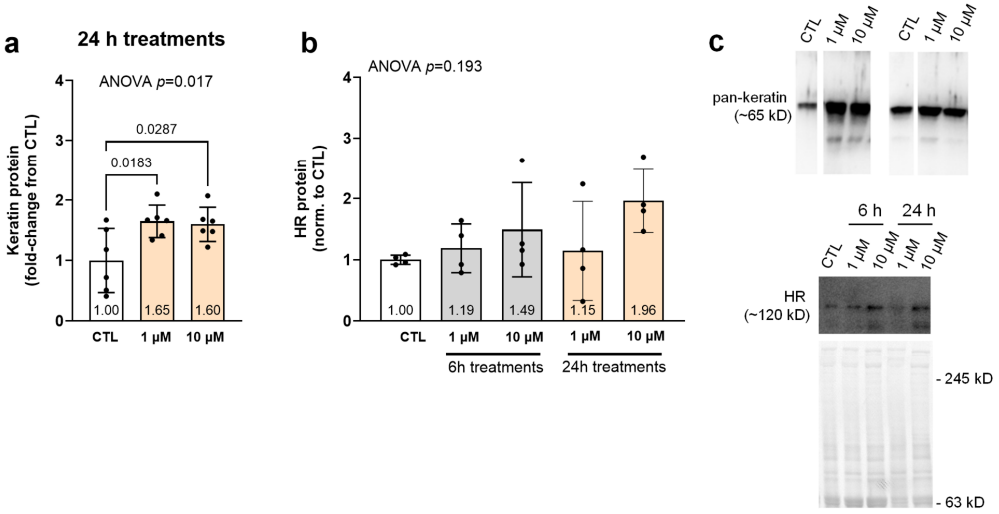


Figure 3. Effects of SPD treatments on pan-keratin and HR protein levels. Legend: These data illustrate pan-keratin (**a**) and HR (**b**) protein levels in lower (1 μM) and/or higher (10 μM) spermidine (SPD) 24 h treated as well as non-treated cells (CTL). (**c**) Contains representative immunoblots. Bars are laid out as mean ± standard deviation values with individual replicate values being presented as dots (n = 4–6 replicates per condition), and mean values are presented at the bottom of each bar. Note, white bars are CTL treatment data and gray and orange bars are 6 h and 24 h SPD treatment data, respectively.

2.4. Effects of 6 and 24 h SPD Treatments on Mitochondrial Outcomes

Figure 4 contains 6 and/or 24 h treatment data for CTL as well as lower (1 μM) and higher (10 μM) SPD doses. JC-1 assays indicated that 24 h 1 μM treatments increased mitochondrial membrane potential compared to CTL ($p < 0.001$), but this effect was not observed with 10 μM treatments (Figure 4a). Despite these mitochondrial function findings, protein levels of TOM20 (a surrogate marker of mitochondrial content) and PGC1-α (a marker of mitochondrial biogenesis) were not significantly affected with 6 and/or 24 h treatments (Figure 4b,c).

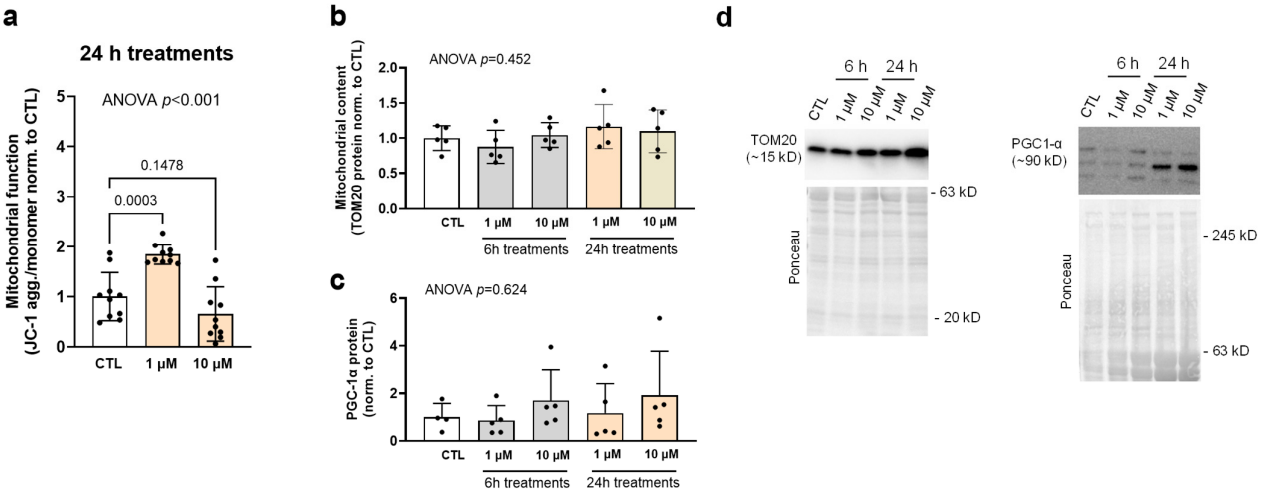


Figure 4. Effects of SPD treatments on mitochondrial markers. Legend: These data illustrate mitochondrial function (i.e., JC-1 assay, (**a**)), as well as protein levels of TOM20 (**b**) and PGC1-α (**c**) in lower (1 μM) and higher (10 μM) spermidine (SPD) 24 h treated as well as non-treated cells (CTL). (**d**) Contains representative immunoblots. Bars are laid out as mean ± standard deviation values with individual replicate values being presented as dots (n = 10 replicates per condition for JC-1 assay and 5–6 per condition for protein markers), and mean values are presented at the bottom of each bar. Note, white bars are CTL treatment data and gray and orange bars are 6 h and 24 h SPD treatment data, respectively.

3. Discussion

These data demonstrate that lower-dose (1–10 μM) SPD treatments alter various cellular outcomes in human primary keratinocytes including mitochondrial function, cellular viability, and pan-keratin production. Transcriptomic data additionally corroborated some of these findings (e.g., increases in cell cycle-related genes suggesting potential increases in viability through enhanced proliferation) while also implicating SPD affects proteostasis and lipid biosynthetic processes. These results support that exogenous SPD may enhance skin health by promoting functional and transcriptomic changes in human keratinocytes. A summary figure of key findings as well as future research directions are presented in Figure 5, and the following paragraphs provide an expanded discussion of our experiments relative to prior literature.

The SPD-induced increase in cell viability, HR gene expression, and enhanced pan-keratin protein production has relevant functional implications for keratinocyte biology. The induction of the HR gene is particularly noteworthy, as the hairless protein functions as a transcriptional corepressor that plays a critical role in hair follicle cycling and keratinocyte differentiation [16]. HR is also essential for the transition from the anagen to catagen phases of the hair cycle and influences the differentiation programs of both interfollicular epidermis and hair follicle keratinocytes [16]. Hence, SPD-induced HR gene expression suggests that SPD may modulate hair follicle biology and potentially influence the balance

between hair growth and regression phases. These findings align with the earlier report by Hynd and Nancarrow demonstrating a critical role of SPD in wool follicle formation [14], further supporting polyamine involvement in follicular development and cycling. The SPD-induced upregulation of pan-keratin production reflects enhanced structural protein synthesis that is fundamental to keratinocyte function. Keratin proteins form the structural backbone of the cytoskeleton in epithelial cells and are essential for maintaining cellular integrity, barrier function, and mechanical resilience of the epidermis [17]. The observed increase in keratin expression suggests that SPD promotes keratinocyte maturation and strengthens cellular barrier properties. Furthermore, enhanced keratin production may contribute to improved wound healing capacity and overall epidermal homeostasis, as keratin proteins are crucial for keratinocyte migration and tissue remodeling processes [17]. These findings are consistent with rodent studies reporting that topical SPD enhances wound repair [12,13]. Collectively, our data in conjunction with prior literature suggest SPD may facilitate the coordination between enhanced keratin synthesis, increased HR gene expression, and cell cycle regulation.

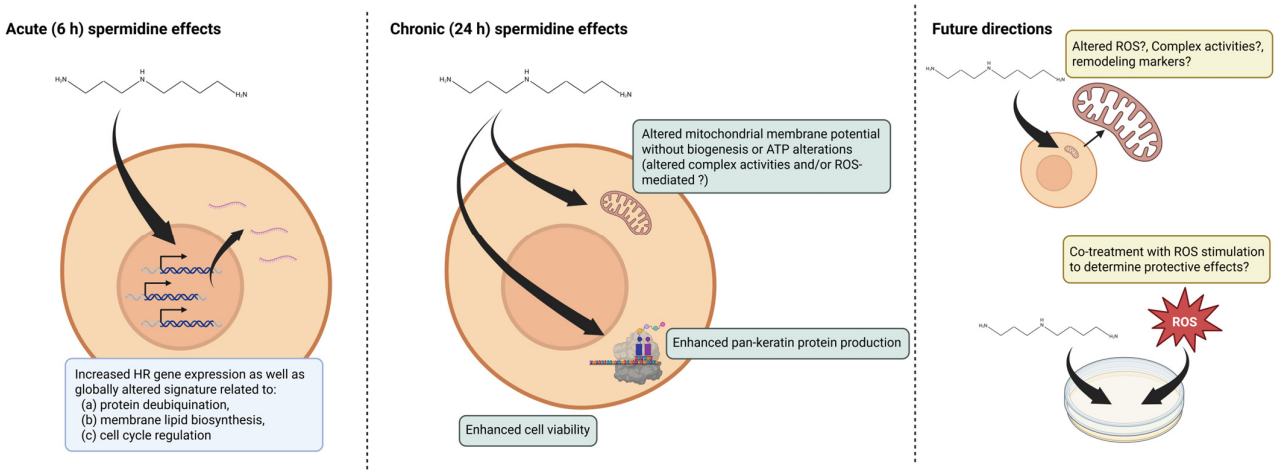


Figure 5. Summary of findings and future directions. Legend: This figure summarizes 6 h (acute) transcriptomic effects as well as 24 h (chronic) effects observed. Future directions based on our findings are also posited. Symbols, "?" indicate hypothesized effects.

Certain mitochondrial-related outcomes were also noteworthy, though complex. While SPD did not affect cellular ATP levels or protein markers indicative of mitochondrial biogenesis or content (i.e., PGC-1α or TOM20), lower dose treatments markedly increased mitochondrial membrane potential, and higher-dose 6 h treatments affected certain transcripts implicated in mitochondrial remodeling (e.g., p62/SQSTM1 and ATG2B) and function (e.g., TOP1MT, MRPL38, and WFS1). Although these collective findings are difficult to reconcile, an enhanced mitochondrial polarization without corresponding ATP changes may indicate that SPD primes keratinocytes for higher metabolic demand. Interestingly, it has been reported that SPD can act to generate reactive oxygen species in microorganisms yet maintain an intricate balance in mitochondrial function through enhanced complex I and II activity [18]. Thus, the potentially enhanced activity of mitochondrial complexes I and II through SPD, which acts to increase electron transport and membrane potential generation, and a potential elevation in ROS production with SPD may activate mild uncoupling mechanisms, allowing cells to maintain optimal mitochondrial membrane potential for cellular signaling and metabolic flexibility without excessive ATP accumulation. These along with the transcriptomic findings also align with prior reports that SPD affects mitochondrial function in aged rodent cardiomyocytes and other cell types [19–21]. However, it should be noted that our hypotheses are highly speculative without further

assays examining some of these key potential mechanisms (e.g., ROS generation assays, mitophagy/autophagy-related assays, etc.), and these intriguing findings in unperturbed keratinocytes warrant further investigation into SPD's specific effects on keratinocyte mitochondria when cells are exposed to certain stressors (e.g., serum starvation, hydrogen peroxide, serum starvation, etc.).

Experimental Considerations

Despite these promising findings, there are limitations to this study. First, this was an exploratory in vitro-only investigation, and while we and others have used micromolar concentrations to examine cellular effects, it is unknown if these culture concentrations emulate what is provided topically or orally (e.g., ~10 mg per oral serving). Additionally, due to limited resources, we only interrogated the transcriptomic effects of 10 μM SPD treatments. However, as 1 μM SPD treatments enhanced mitochondrial membrane potential, it is possible that this dose could affect several mitochondrial-related genes which are not affected by 10 μM SPD treatments. Finally, our RNA array was primarily limited to protein-coding gene expression. As non-coding RNAs have been shown to be involved in polyamine metabolism and keratinocyte biology [22,23], performing RNA-sequencing analyses with future SPD experiments could provide unique additional insight into how SPD affects the transcriptome of keratinocytes.

4. Materials and Methods

4.1. Primary Human Keratinocyte Culture Work

Primary human epidermal keratinocytes (HEKa) from a healthy female donor (30 years old; catalog #: PCS-200-011, lot #: 81117243) as well as dermal cell basal media (catalog #: PCS-200-030) and keratinocyte growth kits (catalog #: PCS-200-040) were purchased from ATCC (Manassas, VA, USA). Documentation provided by the vendor indicated cells were disease-free and mycoplasma contamination was not detected. Cells (passage 0) were first thawed from cryodewar conditions, plated onto a 150 mm plate in 20 mL of complete growth media (i.e., combined basal media and keratinocyte growth kit, denoted as CGM), and incubated at 37 °C, 5% CO_2 atmosphere for 48 h. Cells were then trypsinized using 10 mL of trypsin-EDTA for primary cells for 5 min (ATCC catalog #: PCS-999-003), the reaction was neutralized using trypsin neutralizing solution (ATCC catalog #: PCS-999-004), and the cell solution was transferred to a 50 mL conical tube. The conical tube was centrifuged at 150× *g* for 5 min, the pellet was resuspended in 1 mL of CGM, and cells were counted using a hemacytometer. Thereafter, 100,000 passage 1 cells per mL were seeded onto either 6-well (transcriptomics and immunoblotting) or 96-well culture plates (viability and ATP assays) and cultured to ~90+% confluency through complete growth media changes every 48 h. Once cells reached this level of growth, cells were either treated with CGM + Dulbecco's phosphate-buffered saline (PBS control, or CTL; Dulbecco's PBS was from Thermo Fisher Scientific, Waltham, MS, USA, catalog #: 14190094), CGM + 1 micromolar (μM) SPD (Yuth^{TM} by Compound Solutions; Carlsbad, CA, USA) dissolved in PBS, or CGM + 10 μM SPD dissolved in PBS and treatment times were either 6 h (acute) for transcriptomics or 24 h for the other assays. During treatment days, fresh SPD stock solutions were prepared before each experiment by dissolving spermidine powder in sterile Dulbecco's PBS and used within 2 h, and we at least visually verified that the spermidine was completely solubilized when making these stock solutions. Stock solutions were not reused between experiments to ensure better consistency. The 6 h timepoint for transcriptomic analysis was selected to capture acute transcriptional responses to SPD treatment before secondary effects or mechanisms could potentially alter gene expression changes to treatments. The 24 h timepoint for functional assays (protein expression, cellular

viability, mitochondrial function) was chosen to allow sufficient time for transcript changes to translate into measurable protein and functional alterations. Finally, the micromolar concentrations of SPD were chosen based on prior data examining the effects of 1–10 μM in epithelial stem cells [15] and other cell types [24,25].

4.2. Immunoblotting

Following 24 h CTL, 1 μM SPD, and 10 μM SPD treatments, cells (6-well treatment plates) were removed from incubators, treatment media was decanted, and cells were washed with PBS. Thereafter, 500 μL of general cell lysis buffer (Cell Signaling Technology catalog #: 9803; Danvers, MA, USA) was added, cells were scraped from plates using rubber policemen, and resultant slurries were transferred to 1.7 mL tubes. Tubes were heavily vortexed for ~10 s and then placed at −80 °C until immunoblotting preparation.

On the day of immunoblotting, lysates were removed from −80 °C, thawed, and placed on ice. Lysates were batch-assayed for total protein content using a commercially available BCA protein assay kit (Thermo Fisher Scientific). Lysates were then prepared for Western blotting using 4× Laemmli buffer at 1 μg/μL. Thereafter, 15 μL of prepped samples were loaded onto 4–15% SDS-polyacrylamide gels (Bio-Rad, Hercules, CA, USA) and subjected to electrophoresis (180 V for 50 min) using pre-made 1× SDS-PAGE running buffer (VWR International, Radnor, PA, USA). Proteins were then transferred (200 mA for 2 h) to polyvinylidene difluoride membranes (Bio-Rad), Ponceau stained and imaged to ensure equal protein loading between lanes. Membranes were then blocked for 1 h at room temperature with 5% nonfat milk powder in Tris-buffered saline with 0.1% Tween-20 (TBST; VWR International). Membranes were then incubated overnight at 4 °C on a rocking platform with either a mouse anti-pan keratin antibody solution (Abcam; Waltham, MA, USA; catalog #: ab8068), mouse anti-hairless (HR) antibody solution (Santa Cruz Biotechnology; Dallas, TX, USA; catalog #: sc-514686), or rabbit anti-TOM20 antibody solution (Cell Signaling catalog #: 42406). With each primary antibody solution, antibodies were diluted at 1:1000 in TBST with 5% bovine serum albumin (BSA). The following day, membranes were washed for 15 min in TBST and incubated with either horseradish peroxidase-conjugated anti-mouse or anti-rabbit secondary antibody solutions (1:2000; Cell Signaling) in TBST with 5% BSA at room temperature for 1 h. Membrane development was performed using an enhanced chemiluminescent reagent (Luminata Forte HRP substrate, Millipore Sigma; Burlington, MA, USA; catalog #: ELLUF0100), and band densitometry was performed using a gel documentation system and associated densitometry software (ChemiDoc Touch with Image Lab v6.0.1 software, Bio-Rad). Densitometry values of protein targets were normalized to Ponceau densities. These values were then normalized to the aggregate mean of CTL and data were expressed as fold-change from control treatments.

4.3. Keratinocyte Viability, ATP, and Mitochondrial JC-1 Assays

For cell viability, ATP assays and JC-1 assay cells were grown on three white-walled, clear-bottom 96-well culture plates (Greiner Bio-One; Monroe, NC, USA; catalog #: 655983) and either left untreated (control) or treated for 24 h with 1 μM and 10 μM SPD.

Following the treatment period, one 96-well plate was subjected to a fluorometric cell viability Calcein AM assay (Abcam; catalog #: ab228556) whereby nonfluorescent Calcein AM is converted to green fluorescent Calcein in live cells via acetoxymethyl ester hydrolysis by intracellular esterases. Briefly, treatment media was removed from cells and cells were washed once with PBS. A total of 100 μL of cell dye/Calcein AM solution was then added to each well and the 96-well plate was placed back in the 37 °C incubator for 30 min. Following this 30 min period, the plate was removed from the incubator, placed in a fluorometric microplate reader (Agilent Biotek Synergy H1 hybrid reader, Santa Clara,

CA, USA), and fluorescence was read at Ex/Em = 485/530 nm. All individual readings were normalized to the aggregate mean of CTL and data were expressed as fold-change from control treatments.

A second 96-well plate was subjected to a luminescent ATP assay (Abcam; catalog #: ab113849) following 24 h treatments. Briefly, treatment media was removed from cells and cells were washed once with PBS. Cells were then lysed by adding 50 µL of kit detergent per well and placing the plate on an orbital shaker for 5 min at 500 rpm. Thereafter, 50 µL of kit substrate solution was placed in each well, the plate was placed on an orbital shaker for 5 min at 500 rpm, and luminescence was obtained in a microplate reader (Agilent Biotek Synergy H1 hybrid reader). All individual readings were normalized to the aggregate mean of CTL and data were expressed as fold-change from control treatments.

A third 96-well plate was subjected to a JC-1 assay (Abcam; catalog #: ab113850) following 24 h treatments. Briefly, treatment media was removed from cells and cells were washed once with PBS. Cells were then pulse-treated for 10 min with JC-1 dye (reconstituted in DMSO and diluted 1:100 in CGM) in the 37 °C incubator. Following this 10 min labeling period, cells were removed from the incubator and washed twice with PBS. Cells then recovered in CGM only for a three-hour period before aggregate and monomer readings were obtained on a microplate reader (Agilent Biotek Synergy H1 hybrid reader). All individual readings (aggregate/monomer fluorescence) were normalized to the aggregate mean of CTL and data were expressed as fold-change values from control treatments.

4.4. RNA Isolation, Quantification, and Transcriptomics

Given some of the 24 h results discussed later, we opted to examine the acute transcriptomic effects of 6 h 10 µM SPD treatments. For these experiments, 6-well treatment plates were removed from incubators, treatment media was decanted, cells were washed with PBS, and 500 µL of Trizol (Thermo Fisher Scientific; Waltham, MS, USA) and RNA isolation was performed using chloroform, aqueous phase isolation and isopropanol precipitation per manufacturer's instructions. RNA pellets were resuspended in 30 µL of RNase-free water, concentrations were analyzed in duplicate using a Nanodrop Lite spectrophotometer (Thermo Fisher Scientific).

RNA was then frozen at −80 °C and shipped to a commercial laboratory (North American Genomics, Decatur, GA, USA) on dry ice for transcriptomic analysis using the Clariom S Assay_Human mRNA array (Thermo Fisher Scientific). Prior to analyses, RNA quality was confirmed using a commercially available assay (Agilent, Santa Clara, CA, USA, catalog #: 5067-1511) measured with the Agilent 2100 Bioanalyzer system. Raw transcriptomic data were received as .CEL files and analyzed using the Transcriptome Analysis Console v4.0.2 (Thermo Fisher Scientific). The hg38 (*H. sapiens*) genome was used for annotations, data were normalized using the robust multiarray average (RMA) normalization method, and transcripts are presented as $\log_2$ signal intensities. Significance thresholds were defined a priori as $p < 0.01$ as we have previously implemented with mRNA arrays [26]. We additionally performed Benjamini–Hochberg false discovery rate analysis to determine if any targets possessed FDR-adjusted p-values of <0.05. Bioinformatics using differentially expressed genes (unadjusted $p < 0.01$) was performed using PANTHER v19.0 through the PANTHER GO-Slim Biological Process query. The complete set of mRNA expression data can be found online at figshare.com (https://doi.org/10.6084/m9.figshare.30032773.v1, accessed on 2 September 2025).

4.5. Statistical Analysis

Transcript data were analyzed using the Transcriptome Analysis Console v4.0.2, and the other outcomes were analyzed using one-way ANOVAs with Dunnett's post hoc us-

ing Prism v10.4. Aside from mRNA array data, statistical significance was established at $p < 0.05$ and data reported are displayed as mean ± standard deviation (SD) values throughout.

5. Conclusions

In conclusion, these preliminary screening experiments in non-stressed human keratinocytes suggest that exogenous SPD positively affects various aspects of keratinocyte homeostasis by stimulating transcriptomic and functional alterations. Future research is needed to determine how SPD affects perturbed keratinocytes exposed to stressors such as UV exposure, nutrient deprivation, and oxidative stress.

Author Contributions: Conceptualization, D.A.A. and M.D.R.; methodology, D.A.A., M.L.M. and N.J.K.; software, M.D.R.; validation, D.A.A.; formal analysis, D.A.A. and M.L.M.; investigation, D.A.A., M.L.M. and N.J.K.; resources, M.D.R.; data curation, M.D.R.; writing—original draft preparation, D.A.A. and M.D.R.; writing—review and editing, D.A.A., M.L.M., N.J.K. and M.D.R.; visualization, M.D.R.; supervision, M.D.R.; project administration, M.D.R.; funding acquisition, M.D.R. All authors have read and agreed to the published version of the manuscript.

Funding: This project served as a pre-dissertation study of D.A.A. and N.J.K. who both have interests in determining the physiological effects of polyamines on different cell types. Funding for project reagents was made possible through lab funds provided by the College of Education at Auburn University. Compound Solutions provided SPD but did not have any role in the study design, statistical analyses, or assayed outcomes.

Data Availability Statement: The complete set of mRNA expression data can be found online at figshare.com (https://doi.org/10.6084/m9.figshare.30032773.v1, accessed on 2 September 2025). Other raw data related to the current study outcomes will be provided upon reasonable request by emailing the corresponding author (mdr0024@auburn.edu).

Conflicts of Interest: M.D.R. is a paid consultant for Compound Solutions in accordance with the Auburn University guidance on faculty consulting. His specific role is to advise the company on topics ranging from general assay technologies to study designs on trials the company performs at other institutions. He has no patents nor receives royalties for Yuth™ or any other nutritional supplements sold by Compound Solutions or other companies. The remaining authors declare that the research was conducted in the absence of any commercial or financial relationships that could be construed as a potential conflict of interest.

References

1. Diegel, K.L.; Danilenko, D.M.; Wojcinski, Z.W. The integumentary system. In *Fundamentals of Toxicologic Pathology*; Academic Press: Cambridge, MA, USA, 2018; pp. 791–822. Available online: https://www.ncbi.nlm.nih.gov/books/NBK430685/?report=reader (accessed on 21 September 2025).
2. Lopez-Ojeda, W.; Pandey, A.; Alhajj, M.; Oakley, A.M. Anatomy, Skin (Integument). In *StatPearls*; StatPearls Publishing: Petersburg, FL, USA, 2025.
3. Zhang, B.; Chen, T. Local and systemic mechanisms that control the hair follicle stem cell niche. *Nat. Rev. Mol. Cell Biol.* **2024**, *25*, 87–100. [CrossRef]
4. Ramos-Molina, B.; Queipo-Ortuno, M.I.; Lambertos, A.; Tinahones, F.J.; Penafiel, R. Dietary and Gut Microbiota Polyamines in Obesity- and Age-Related Diseases. *Front. Nutr.* **2019**, *6*, 24. [CrossRef]
5. Zou, D.; Zhao, Z.; Li, L.; Min, Y.; Zhang, D.; Ji, A.; Jiang, C.; Wei, X.; Wu, X. A comprehensive review of spermidine: Safety, health effects, absorption and metabolism, food materials evaluation, physical and chemical processing, and bioprocessing. *Compr. Rev. Food Sci. Food Saf.* **2022**, *21*, 2820–2842. [CrossRef]
6. Scalabrino, G.; Ferioli, M.E. Polyamines in mammalian ageing: An oncological problem, too? A review. *Mech. Ageing Dev.* **1984**, *26*, 149–164. [CrossRef]
7. Senekowitsch, S.; Wietkamp, E.; Grimm, M.; Schmelter, F.; Schick, P.; Kordowski, A.; Sina, C.; Otzen, H.; Weitschies, W.; Smollich, M. High-Dose Spermidine Supplementation Does Not Increase Spermidine Levels in Blood Plasma and Saliva of Healthy Adults: A Randomized Placebo-Controlled Pharmacokinetic and Metabolomic Study. *Nutrients* **2023**, *15*, 1852. [CrossRef]

8. Eisenberg, T.; Knauer, H.; Schauer, A.; Buttner, S.; Ruckenstuhl, C.; Carmona-Gutierrez, D.; Ring, J.; Schroeder, S.; Magnes, C.; Antonacci, L.; et al. Induction of autophagy by spermidine promotes longevity. *Nat. Cell Biol.* **2009**, *11*, 1305–1314. [CrossRef]
9. Minois, N.; Carmona-Gutierrez, D.; Bauer, M.A.; Rockenfeller, P.; Eisenberg, T.; Brandhorst, S.; Sigrist, S.J.; Kroemer, G.; Madeo, F. Spermidine promotes stress resistance in Drosophila melanogaster through autophagy-dependent and -independent pathways. *Cell Death Dis.* **2012**, *3*, e401. [CrossRef]
10. Madeo, F.; Eisenberg, T.; Pietrocola, F.; Kroemer, G. Spermidine in health and disease. *Science* **2018**, *359*, eaan2788. [CrossRef]
11. Liang, Y.; Piao, C.; Beuschel, C.B.; Toppe, D.; Kollipara, L.; Bogdanow, B.; Maglione, M.; Lutzkendorf, J.; See, J.C.K.; Huang, S.; et al. eIF5A hypusination, boosted by dietary spermidine, protects from premature brain aging and mitochondrial dysfunction. *Cell Rep.* **2021**, *35*, 108941. [CrossRef]
12. Ito, D.; Ito, H.; Ideta, T.; Kanbe, A.; Ninomiya, S.; Shimizu, M. Systemic and topical administration of spermidine accelerates skin wound healing. *Cell Commun. Signal* **2021**, *19*, 36. [CrossRef]
13. Jouyban, K.; Mohammad Jafari, R.; Charkhpour, M.; Rezaei, H.; Seyfinejad, B.; Manavi, M.A.; Tavangar, S.M.; Dehpour, A.R. Spermidine Exerts Protective Effects in Random-Pattern Skin Flap Survival in Rats: Possible Involvement of Inflammatory Cytokines, Nitric Oxide, and VEGF. *Aesthetic Plast. Surg.* **2024**, *48*, 3500–3509. [CrossRef]
14. Hynd, P.I.; Nancarrow, M.J. Inhibition of polyamine synthesis alters hair follicle function and fiber composition. *J. Investig. Dermatol.* **1996**, *106*, 249–253. [CrossRef]
15. Ramot, Y.; Tiede, S.; Biro, T.; Abu Bakar, M.H.; Sugawara, K.; Philpott, M.P.; Harrison, W.; Pietila, M.; Paus, R. Spermidine promotes human hair growth and is a novel modulator of human epithelial stem cell functions. *PLoS ONE* **2011**, *6*, e22564. [CrossRef]
16. Panteleyev, A.A.; Paus, R.; Ahmad, W.; Sundberg, J.P.; Christiano, A.M. Molecular and functional aspects of the hairless (hr) gene in laboratory rodents and humans. *Exp. Dermatol.* **1998**, *7*, 249–267. [CrossRef]
17. Pan, X.; Hobbs, R.P.; Coulombe, P.A. The expanding significance of keratin intermediate filaments in normal and diseased epithelia. *Curr. Opin. Cell Biol.* **2013**, *25*, 47–56. [CrossRef]
18. Han, X.; Shangguan, J.; Wang, Z.; Li, Y.; Fan, J.; Ren, A.; Zhao, M. Spermidine Regulates Mitochondrial Function by Enhancing eIF5A Hypusination and Contributes to Reactive Oxygen Species Production and Ganoderic Acid Biosynthesis in Ganoderma lucidum. *Appl. Environ. Microbiol.* **2022**, *88*, e0203721. [CrossRef]
19. Song, N.; Ji, E.; Yu, J.E.; Choi, K.H.; Kim, D.H.; Song, J.M.; Kang, D.H.; Song, J.K.; Yu, J.; Kim, K.; et al. Spermidine Enhances Mitochondrial Function and Mitigates Aortic Valve Calcification: Implications for DNA Methyltransferase-1 Activity. *JACC Basic Transl. Sci.* **2025**, *10*, 345–366. [CrossRef]
20. Messerer, J.; Wrede, C.; Schipke, J.; Brandenberger, C.; Abdellatif, M.; Eisenberg, T.; Madeo, F.; Sedej, S.; Muhlfeld, C. Spermidine supplementation influences mitochondrial number and morphology in the heart of aged mice. *J. Anat.* **2023**, *242*, 91–101. [CrossRef]
21. Wang, J.; Li, S.; Wang, J.; Wu, F.; Chen, Y.; Zhang, H.; Guo, Y.; Lin, Y.; Li, L.; Yu, X.; et al. Spermidine alleviates cardiac aging by improving mitochondrial biogenesis and function. *Aging* **2020**, *12*, 650–671. [CrossRef]
22. Juarez-Vicuna, Y.; Ruiz-Ojeda, D.; Gonzalez-Ramirez, J.; Flores-Balderas, X.; Springall, R.; Sanchez-Munoz, F.; Guzman-Martin, C.A. LncRNA MALAT1 in Keratinocyte function: A review of recent advances. *Noncoding RNA Res.* **2024**, *9*, 594–601. [CrossRef]
23. Rossi, M.N.; Fiorucci, C.; Mariottini, P.; Cervelli, M. Unveiling the hidden players: Noncoding RNAs orchestrating polyamine metabolism in disease. *Cell Biosci.* **2024**, *14*, 84. [CrossRef] [PubMed]
24. Ghisalberti, C.A.; Morisetti, A.; Bestetti, A.; Cairo, G. Potent trophic activity of spermidine supramolecular complexes in in vitro models. *World J. Biol. Chem.* **2013**, *4*, 71–78. [CrossRef]
25. Wei, Z.X.; Cai, L.; Zhao, X.M.; Jiang, X.R.; Li, X.L. Effects of Spermidine on Cell Proliferation, Migration, and Inflammatory Response in Porcine Enterocytes. *Front. Biosci.* **2022**, *27*, 194. [CrossRef]
26. Sexton, C.L.; Godwin, J.S.; McIntosh, M.C.; Ruple, B.A.; Osburn, S.C.; Hollingsworth, B.R.; Kontos, N.J.; Agostinelli, P.J.; Kavazis, A.N.; Ziegenfuss, T.N.; et al. Skeletal Muscle DNA Methylation and mRNA Responses to a Bout of Higher versus Lower Load Resistance Exercise in Previously Trained Men. *Cells* **2023**, *12*, 263. [CrossRef]

Disclaimer/Publisher's Note: The statements, opinions and data contained in all publications are solely those of the individual author(s) and contributor(s) and not of MDPI and/or the editor(s). MDPI and/or the editor(s) disclaim responsibility for any injury to people or property resulting from any ideas, methods, instructions or products referred to in the content.